CHARACTERISTICS OF BRAKED, LOCKED, AND FREE-WHEELING TWO- AND THREE-BLADED PROPELLERS

THESIS BY

Frank J. Malina
and
William W. Jenney

In partial fulfillment of the requirements for the Degree of Master of Science in Aeronautical Engineering

California Institute of Technology
Pasadena, California
1936

Characteristics of Braked, Locked, and Free-Wheeling Two- and Three-bladed Propellers

INTRODUCTION

The use of multi-engined aircraft has introduced the problem of aircraft performance when one or more power units have either become unusable or voluntarily shut down during cruising flight. If the use of the engine is to be discontinued because of mechanical failure, the desirable procedure is obviously to stop it altogether, so as to prevent possible destruction to the engine. This can be accomplished by locking the propeller, by a free-wheeling arrangement, or by feathering a variable pitch propeller. If the use of the engine is to be discontinued merely to reduce fuel consumption, the propeller may be allowed to turn the engine, in which case the propeller is braked by a torque equal to the friction of the engine.

Another recent development connected with braked propellers is the fact that the variable pitch propeller now offers the possibility of using the large increment in drag at low blade angles of braked and free-wheeling propellers for reduction in landing speed or landing run of clean, highly powered, multi-engined aircraft.

It was the purpose of the present investigation to provide information not already made available by researches listed under the references at the end of this paper. Therefore the following thesis will be concerned chiefly with the three-bladed propeller and its effect on

airplane characteristics, the two-bladed propeller being used principally for comparison purposes with other available data. The tests were performed at model scale, but their acceptance as applicable to full scale is supported by the favorable comparisons made in Reference 5.

APPARATUS

The tests were made in the closed working section of the ten-foot tunnel of the Guggenheim Aeronautics Laboratory, California Institute of Technology. (See Fig. 1 and Fig. 2) using a one-sixth scale model, the dimensions of which are shown in Fig. 3. The propeller was 18 inches in diameter, the tips having been cut off of the propeller used in GALCIT Report #148. The blades were of aluminum alloy made to the specifications of the Hamilton Standard 1A1-0 blade. The blade could be adjusted to any pitch angle in a steel, split-type hub.

For a detailed description of the apparatus and method of determining the various parameters required in calculating the propeller coefficients and airplane characteristics, see References 2 and 5.

Several minor changes in testing set-up were, however, made. To insure closer cooperation between various members of the testing group the model instrument table was moved to the tunnel balance floor. The ammeter in the model power circuit was also moved to the same location. This change necessitated the use of much longer instrument leads and the nearness of the model power leads to the instrument leads required an investigation of a possible electrical effect. No effect was, however, detectable.

In the timing circuit of the model propeller (See Fig. 4) the contactor power was taken from the D.C. house line through a transformer giving forty volts instead of the twenty-four volts used before from storage batteries.

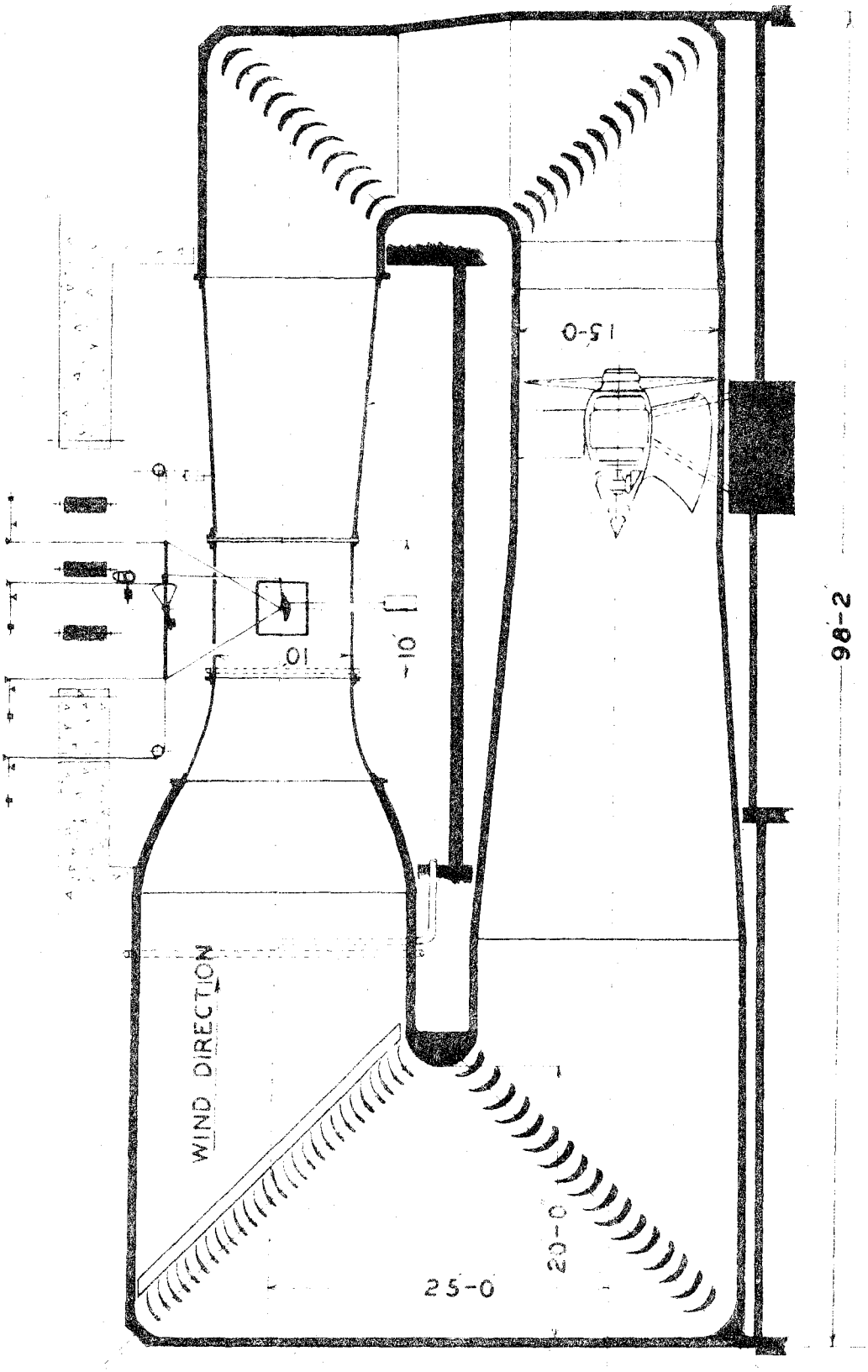

VERTICAL SECTION THROUGH 10' WIND TUNNEL

GUGGENHEIM AERONAUTICAL LABORATORY
CALIFORNIA INSTITUTE OF TECHNOLOGY
PASADENA

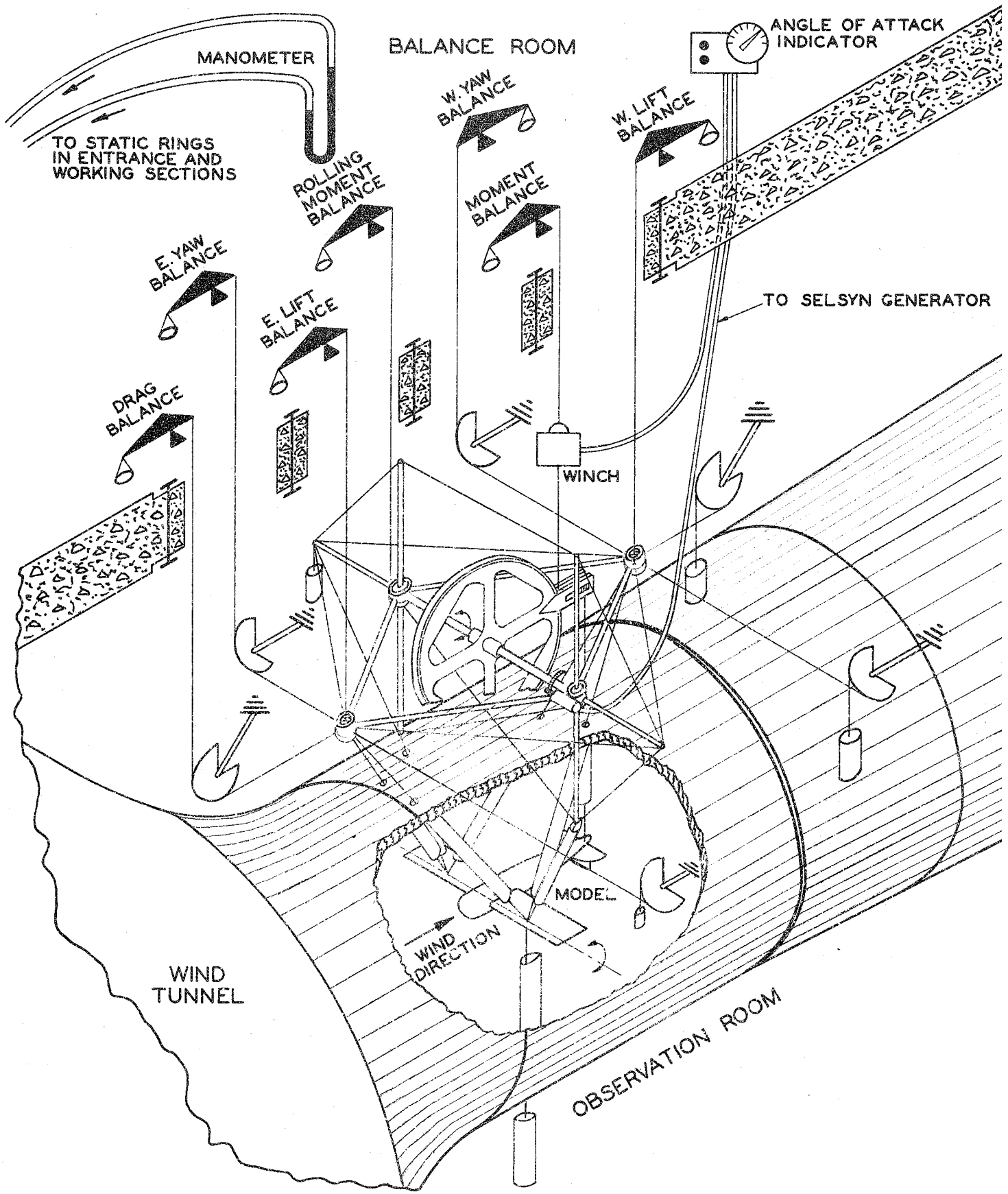

SIX COMPONENT SETUP FOR TEN FOOT WIND TUNNEL TESTS
AT GUGGENHEIM AERONAUTICS LABORATORY
CALIFORNIA INSTITUTE OF TECHNOLOGY

FIG. 2

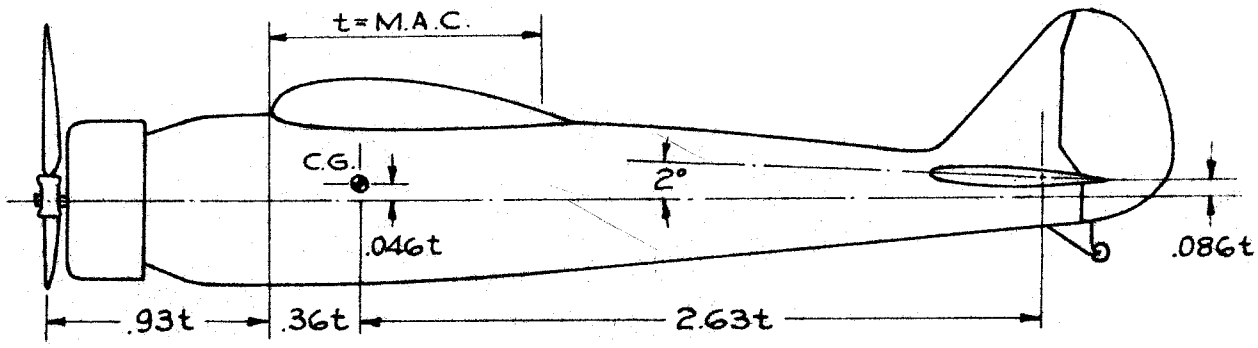

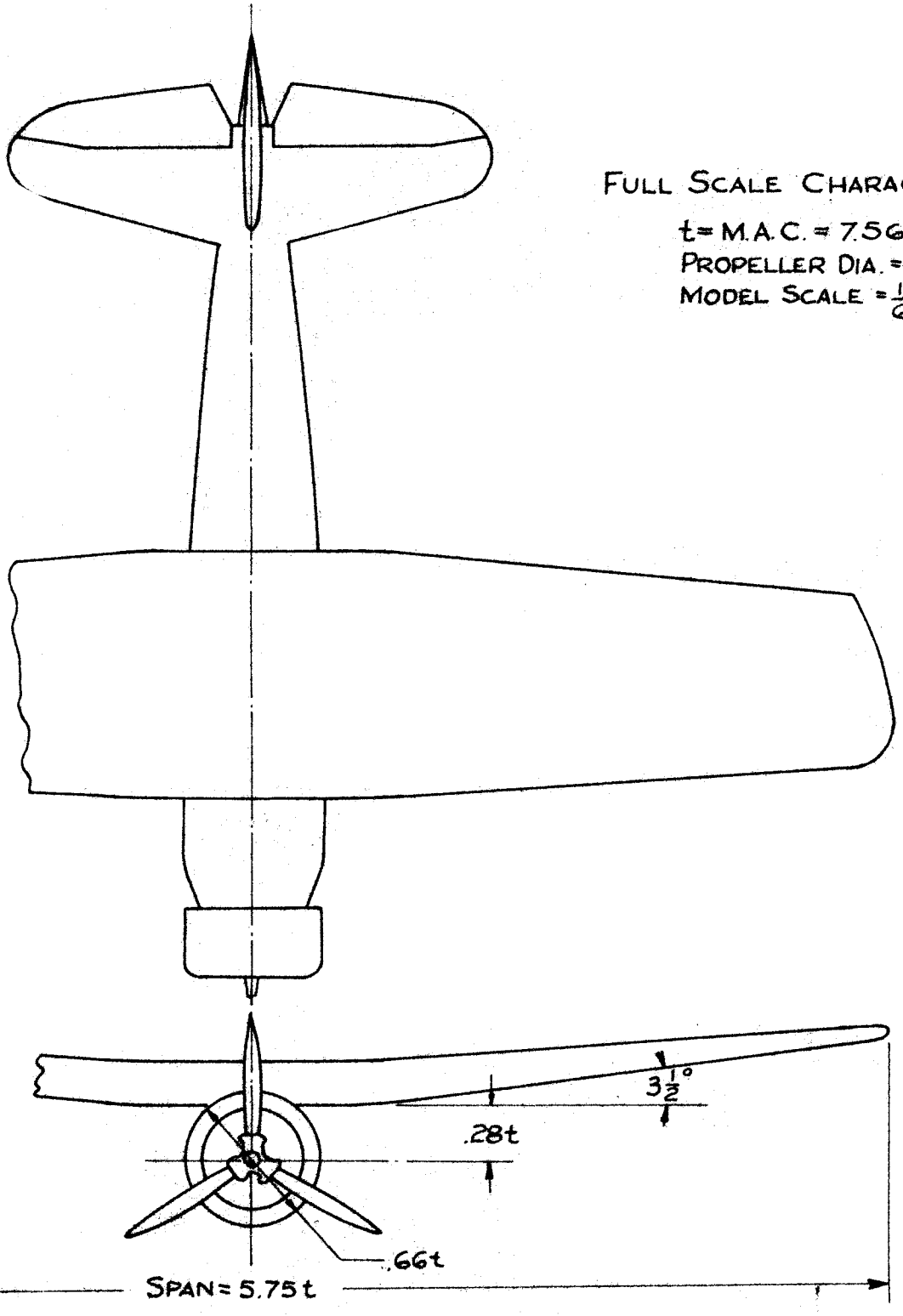

FULL SCALE CHARACTERISTICS

t=M.A.C.=7.56 FT.
PROPELLER DIA.=9FT
MODEL SCALE=$\frac{1}{6}$

SCALE DRAWING OF MODEL USED IN TESTS

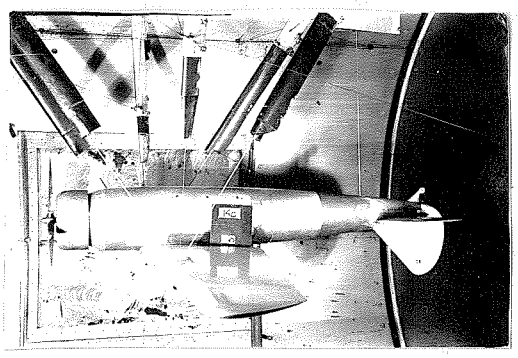

SIDE VIEW

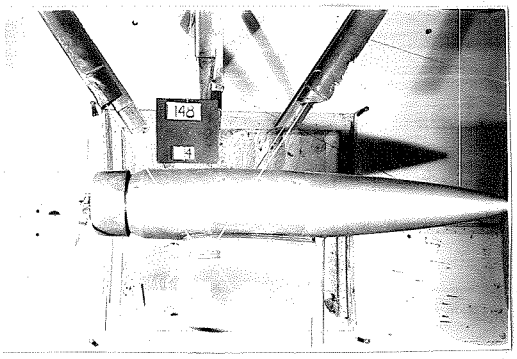

SIDE VIEW

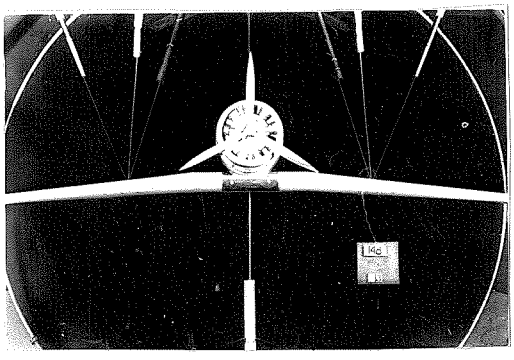

FRONT VIEW

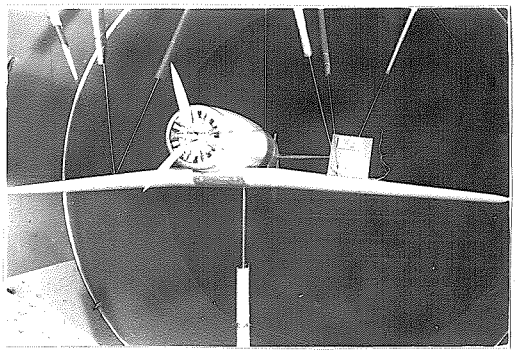

THREE-QUARTER VIEW

NOTE: Pictures show propeller before tips were cut off.

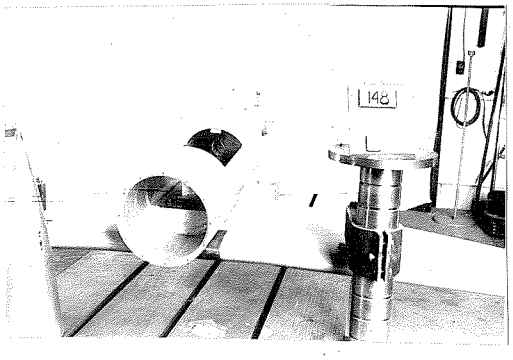

MODEL DISASSEMBLED

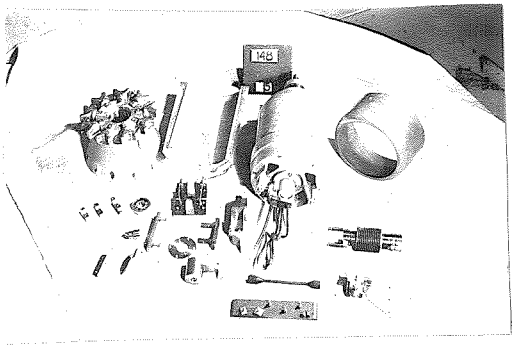

MOTOR AND MODEL PARTS

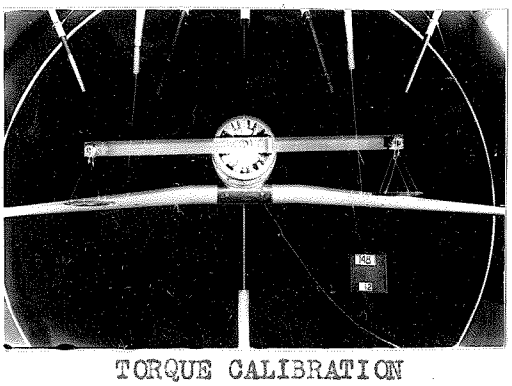

TORQUE CALIBRATION

Figure 5

Photographs in Fig. 5 show views of the model, model parts , and torque calibration arrangement.

NOTATION

The various coefficients used for presenting the data are defined as follows:

$J = V/nD$

$T_c = T/\rho V^2 D^2$

$Q_c = Q/\rho V^2 D^3$

$Q_n = Q_c(V/nD) = (17200\ Q_f/\text{propeller rpm.})/\sigma D^4 \times \text{mph.}$

Q_f = Friction torque (ft.-lb.)

Where:

T = Effective thrust (lbs) (cf. Ref. 5). Negative sign indicates force in the direction of a drag force.

Q = Torque (ft.-lb.) Negative sign indicates propeller turning engine.

V = Velocity (ft./sec.)

D = Propeller diameter (ft.)

β = Blade angle at 0.75 radius (degrees)

h = Altitude (ft)

ρ = Air density (slugs/cu.ft.)

σ = Relative air density

n = Revolutions per second of propeller

N = Propeller rpm.

N_e = Engine crankshaft rpm.

Δ = Engine displacement (cu.in.)

For the presentation of airplane characteristics the usual coefficients C_L, C_D, C_M and α are used.

BRAKED PROPELLER

The condition of braking action of a propeller is obtained when the rate of advance has become so high that thrust and torque have both become negative. This condition can be brought about on existing single-engined aircraft during a fast glide and on multi-engined aircraft by reducing the revolutions of one engine below that of other units. If the propeller is allowed to turn a dead-engine, it will be braked by a torque equal to the friction torque of the engine at specified conditions.

To obtain data for the braked propeller curves, the model induction motor was used as an electrical brake by appropriate selection of supply power frequency. The first tests were performed with the two-bladed propeller for the purpose of obtaining a comparison with the data presented in N.A.C.A. T.R. #464 and of extending these data to higher blade angles. The results are shown in Figure 6. As the model configuration used for these tests differed largely from that of a monoplane wing with nacelle in position C (loc. cit.), the comparison should be regarded as merely qualitative. The points shown in Fig. 6 and Fig. 7 were obtained directly from experimental data without crossplotting or cross-fairing and show very little experimental scatter.

The extension to higher blade angles shows that the negative torque curves become much steeper, reaching greater negative torques, and that the negative thrust curves become less steep with corresponding decrease in negative thrust.

In Fig. 7 are presented the characteristics of the three-bladed propeller for blade angles varying from 12° to 50°. The curves very closely resemble those of the two-bladed propeller, differing primarily

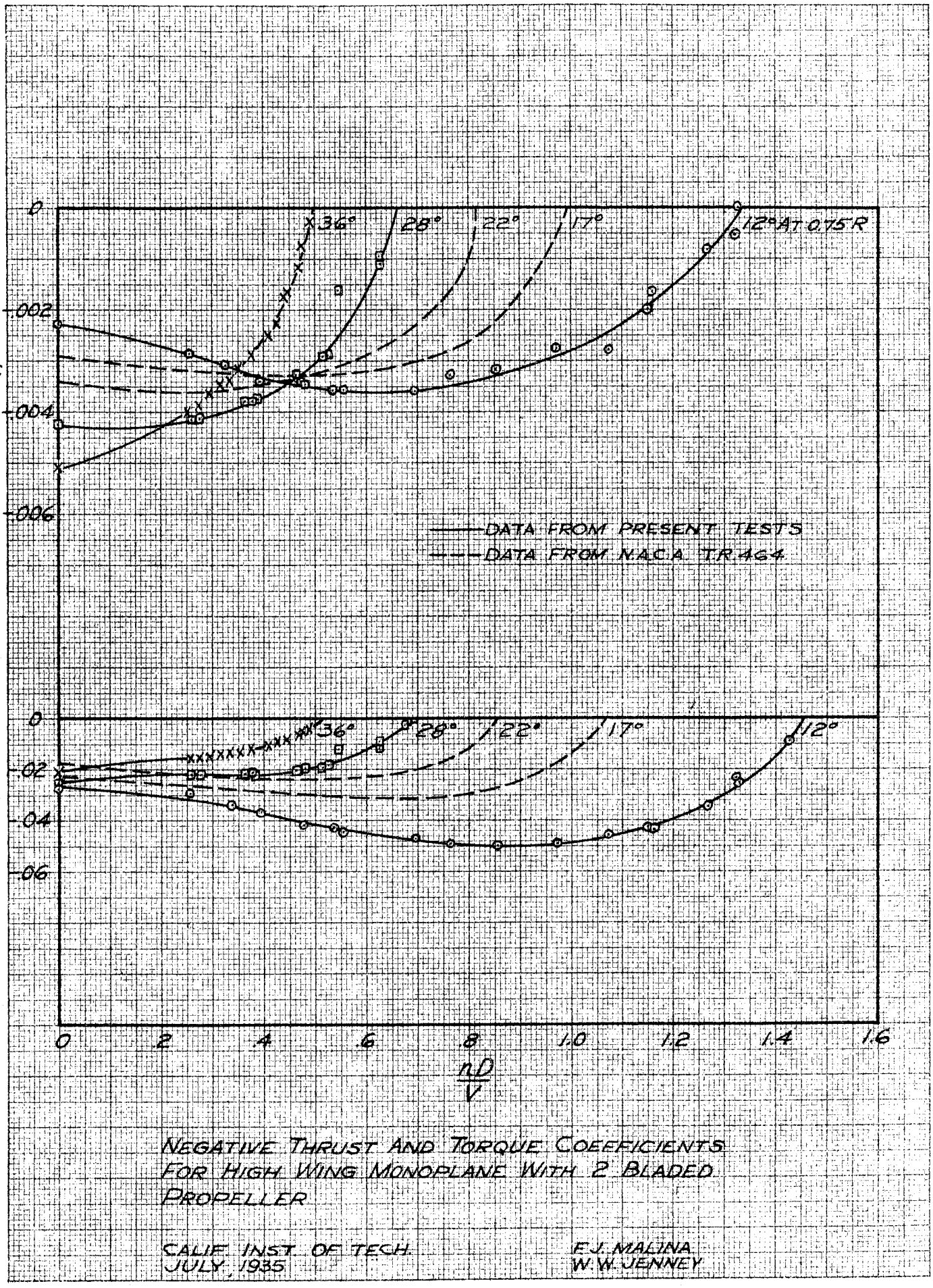

NEGATIVE THRUST AND TORQUE COEFFICIENTS FOR HIGH WING MONOPLANE WITH 2 BLADED PROPELLER

CALIF. INST. OF TECH.
JULY, 1935

F. J. MALINA
W. W. JENNEY

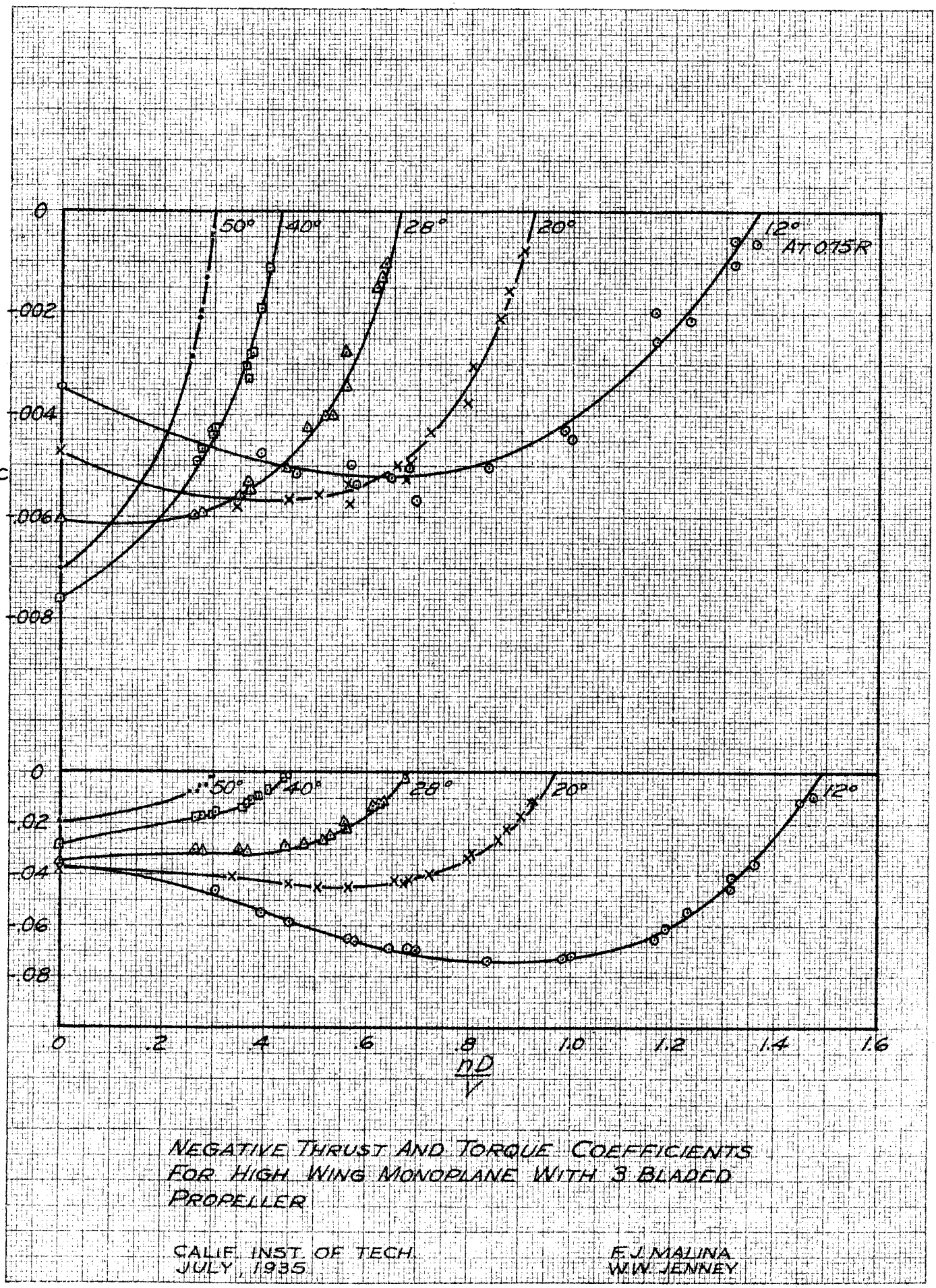

NEGATIVE THRUST AND TORQUE COEFFICIENTS FOR HIGH WING MONOPLANE WITH 3 BLADED PROPELLER

CALIF. INST. OF TECH.
JULY, 1935

E.J. MALINA
W.W. JENNEY

in the greater values of negative torque and thrust reached for a given blade angle.

For both the two- and three-bladed propeller the region between nD/V equal to 0 and 0.25 could not be covered because of the excessively low rotational speeds or excessively high wind tunnel velocities required. The points for nD/V equal to 0 were obtained from locked propeller data.

The determination from the above curves of the negative torque and thrust for a propeller restrained to a predetermined rpm. by regulation of engine power requires only a knowledge of the forward velocity, propeller diameter, and blade angle. The determination of the negative thrust caused by a propeller overcoming the friction torque of a dead-engine requires in addition inform ation with regard to the friction characteristics of the engine.

Through the cooperation of the Army, Navy, and several engine manufacturers, the authors were able to collect friction horsepower curves for a considerable number of radial engines ranging from 150 to nearly 1000 hp. In Fig. 8 these friction hp. curves have been replotted against rpm . The original friction curves obtained from various sources and a table of manufacturers data (at present considered confidential) on the engines referred to numerically in Fig. 8 may be found in the copy of the thesis kept in the file of GALCIT wind tunnel reports.

Flight tests indicate that the rotational speeds of all normal propellers turning a dead-engine on a multi-engine airplane range from 35% to 50% of rated rpm. (Ref.3) To obtain the friction horsepower in this range it was necessary to extrapolate many of the curves of Fig. 8 towards the origin. The accuracy of such an extrapolation naturally depends very largely on individual judgment, and its validity, therefore, cannot be definitely determined until more engine test data become available.

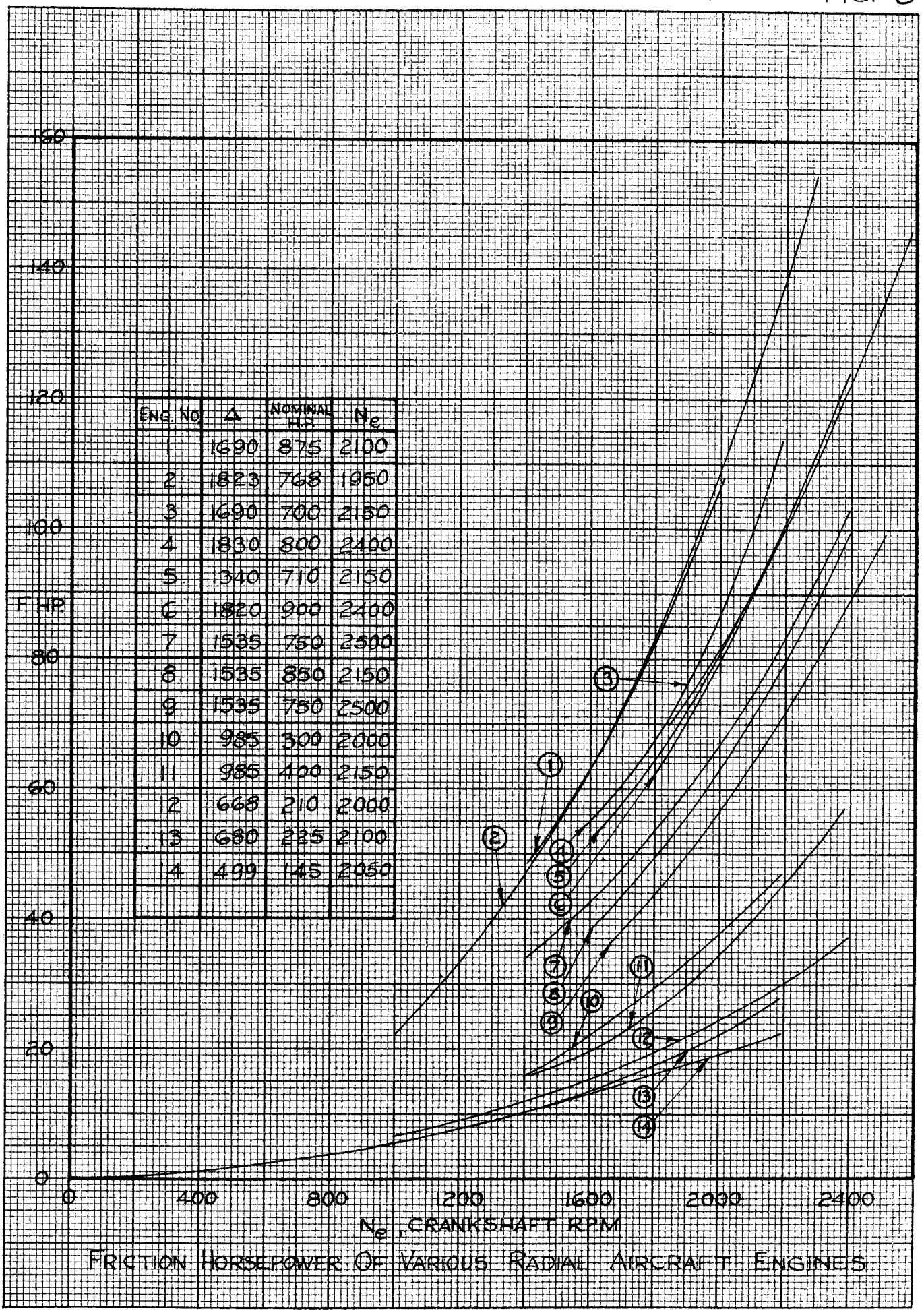

Eng. No.	Δ	Nominal H.P.	N_e
1	1690	875	2100
2	1823	768	1950
3	1690	700	2150
4	1830	800	2400
5	1340	710	2150
6	1820	900	2400
7	1535	750	2500
8	1535	850	2150
9	1535	750	2500
10	985	300	2000
11	985	400	2150
12	668	210	2000
13	680	225	2100
14	499	145	2050

FRICTION HORSEPOWER OF VARIOUS RADIAL AIRCRAFT ENGINES

Investigations made on the friction horsepower of aircraft engines reveal that in general:

1. F.H.P. increases with rpm.
2. " " " displacement
3. " " " compression ratio (questionable)
4. " decreases " throttle opening
5. " " " increasing temperature
6. " depends greatly on viscosity of oil used.
7. " " " " mechanical condition of engine

For an engine of given design the friction hp. of a dead-engine will depend principally on the rpm. and the oil temperature. The temperature in turn in dependant on the altitude at which the aircraft is flying.

The points shown in Fig. 9 were obtained by taking the avarage slope of the Q_f vs. engine rpm. curves determined from Fig. 8 for the range of rpm. from 35% to 50% of the rated rpm. For the curve faired through these points, an empirical formula was developed which should give an indication of the friction torque to be encountered in dead-engines of various displacements. A correction for altitude has also been included. The data for this were obtained from engine tests on a Wright R-1820-F-2 engine covering the range of altitudes shown in Fig. 10. The formula is of the form:

$$Q_f/N_e = 2.2\Delta(0.3\Delta + 0.0143h - 6)10^{-7}$$

The original empirical equation for Q_f/N_e obtained from friction hp. data (Fig.9) has been multiplied by the factor 2.2 . This factor was included to bring about closer agreement of rpm. with flight test rpm. The factor was selected on the basis of flight test data available. A more comprehensive amount of flight test data is necessary to ascertain this factor more positively. The factor enters into the equation because of differences in

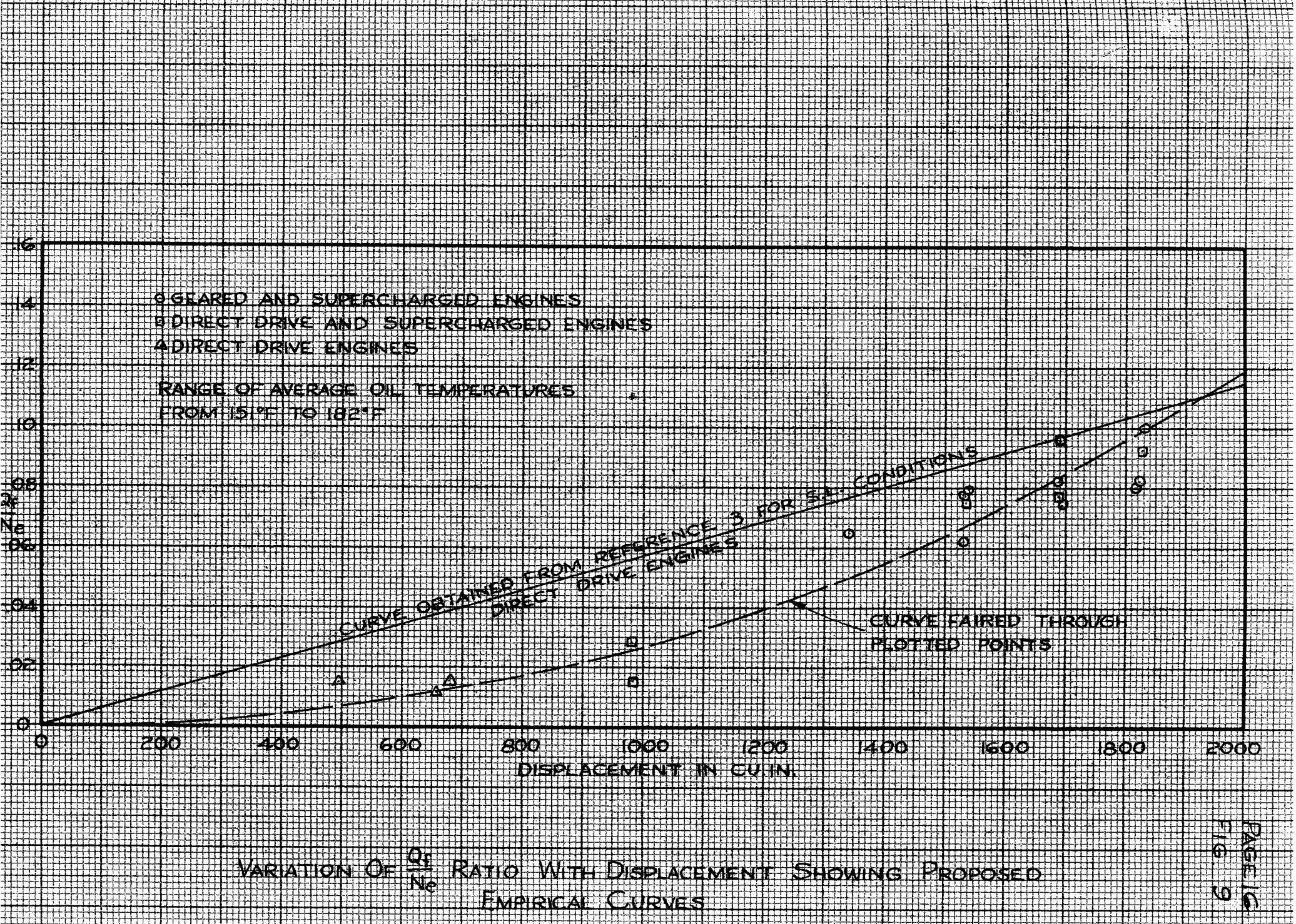

VARIATION OF $\frac{Q_f}{N_e}$ RATIO WITH DISPLACEMENT SHOWING PROPOSED EMPIRICAL CURVES

FIG. 6

PAGE 15

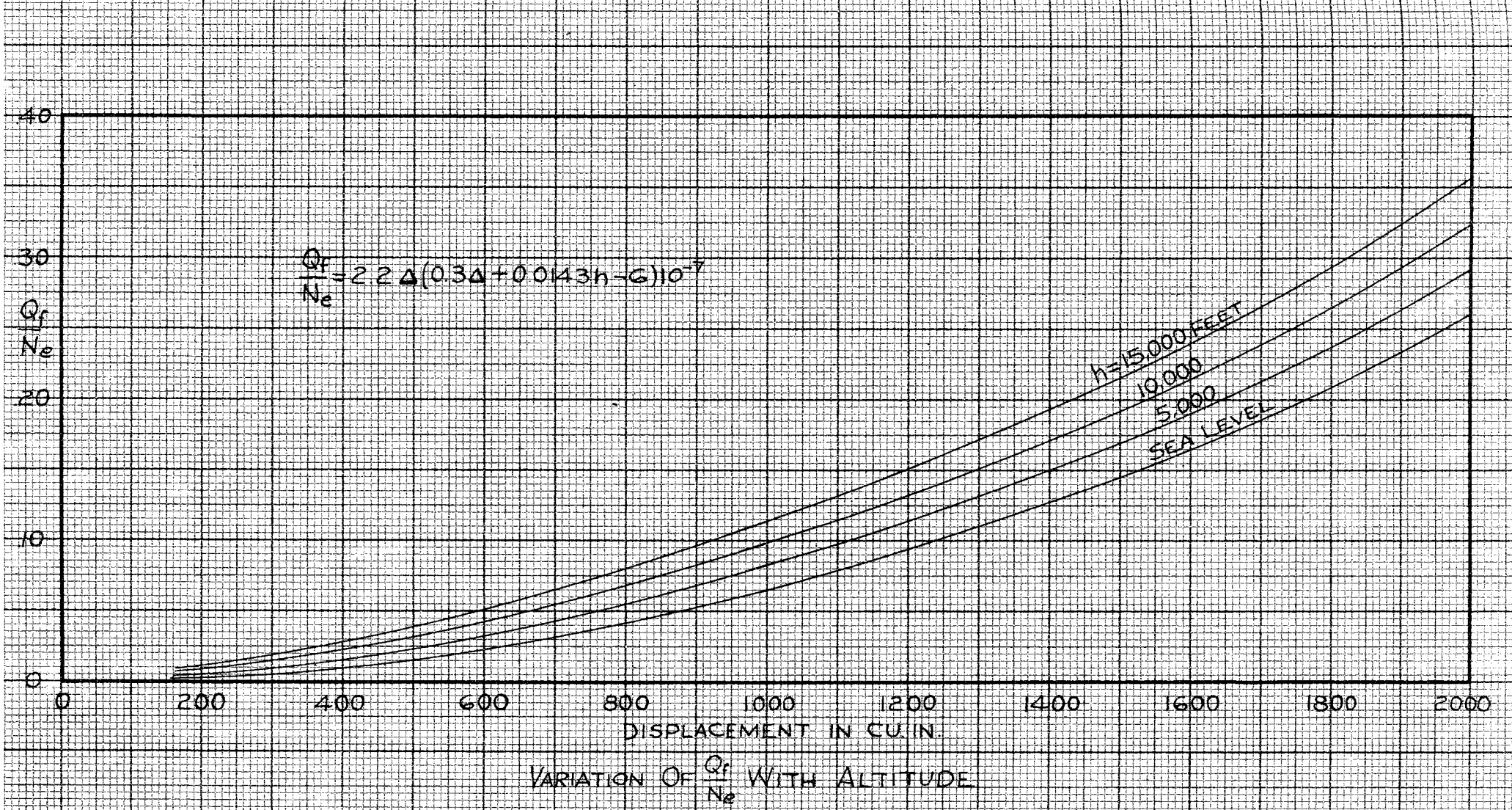

VARIATION OF $\frac{Q_f}{N_e}$ WITH ALTITUDE

operating conditions in flight from those encountered on the engine test stand.

In the ratio Q_f/N_e, N_e refers to the rpm. of the engine crankshaft. After obtaining Q_f/N from an engine curve or from the above equation, the following method taken from Reference 3 can be used to determine negative thrust:

Estimate flight velocity.

Calculate Q_n or Q_c (See Pg. 3). Calculation of Q_c requires an assumption for N.

For three-bladed propellers obtain T_c from Fig. 11 which has been obtained from Fig. 7 by cross-plotting. For two-bladed propellers use the data of Fig. 6 or the cross-plot given in Ref. 3. If Q_c has been determined, Fig 6 or Fig. 7 is more convenient.

Since Q_f/N_e was assumed constant over the range to be considered there is no need to correct the n obtained from nD/V in Fig. 11. If, however, N was assumed to obtain Q_f and hence Q_c, it is necessary to check the assumption.

Fig. 9 shows a curve corresponding to the equation for Q_f/N_e given in Reference 3. Since it falls higher than the points, which were calculated from experimental friction data, it appears conservative for three-bladed propellers for blade angles of 28° and greater, while it may be the opposite for blade angles below 28° due to the peak in the curves below 28° (See Fig. 11) and the possibility of falling on the right hand side of the peak with high values of Q_n.

In Table II the results obtained by using the method of this thesis and of Ref. 3 are compared with flight test data.

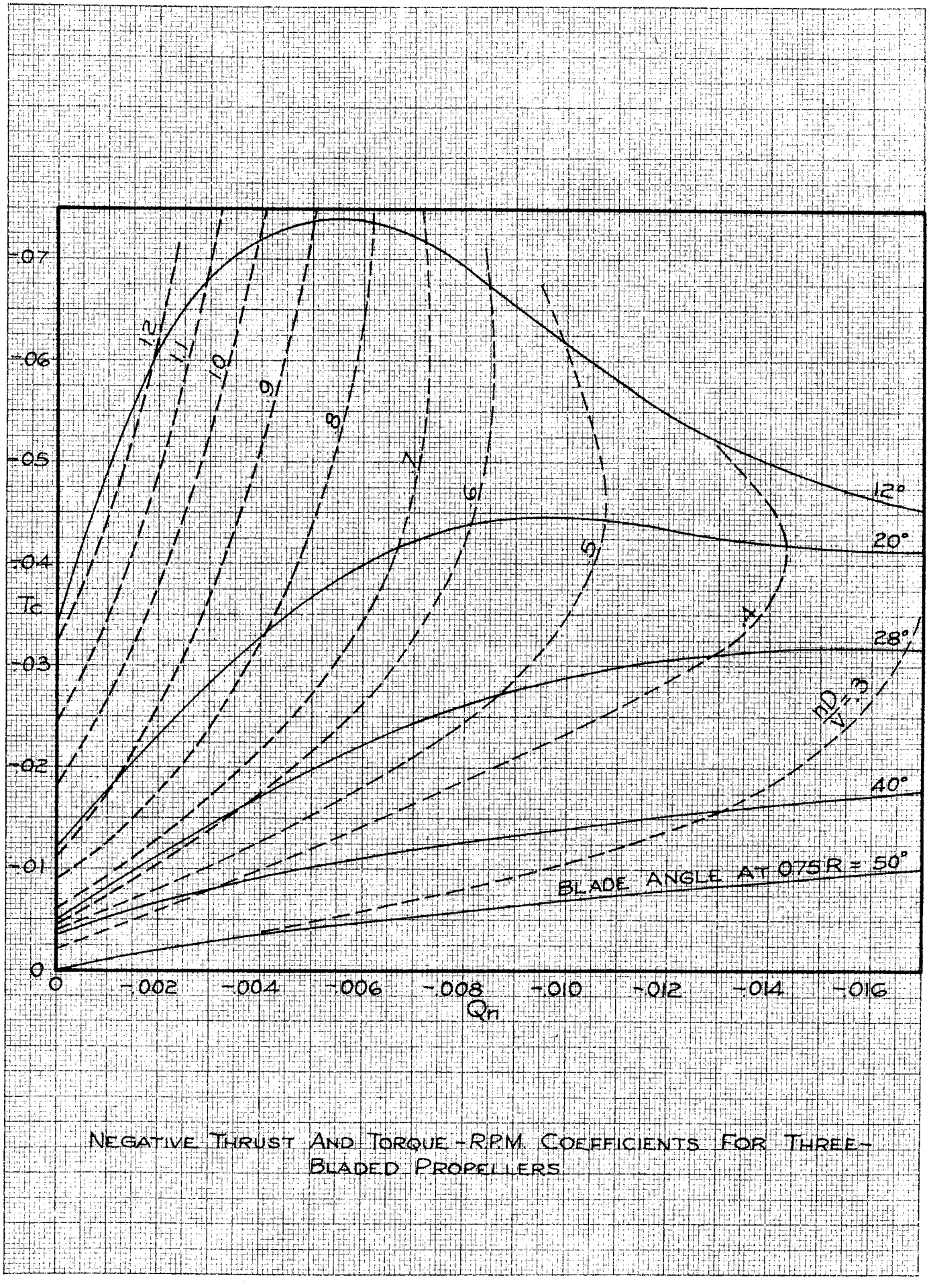

NEGATIVE THRUST AND TORQUE - R.P.M. COEFFICIENTS FOR THREE-BLADED PROPELLERS

AIRPLANE	D	β @ .75R	ALT.	V	Δ	GEAR RATIO	σ	METHOD	$\frac{Q_f}{N}$	Q_n	T_c	$\frac{nD}{V}$	CALC. R.P.M.	FLIGHT TEST R.P.M.	
BOEING YB-9	11.5	27.7	6800	112	1860	.667	.816	M-J	.398	.00426	.0180	.55	758	720	THREE BLADED PROPELLER
								D	.217	.00233	.0135	.60	770		
BOEING YIB-9	9.83	21.5	3500	101	1570	.714	.902	M-J	.248	.00495	.031	.75	950	950	
								D	.161	.00327	.024	.76	960		
DOUGLAS XO-35	9.83	21.5	5500	110	1570	.714	.848	M-J	.262	.00561	.030	.72	993	800	
								D	.167	.00331	.025	.75	1030		
BOEING 247	9	23	2000	110	1340	1	.943	M-J	.125	.00316	.014	.77	828		
								D	.079	.00200	.017	.74	800		
DOUGLAS DC-2	11	23	9500	113	1820	.687	.750	M-J	.394	.00550	.029	.69	906	1000	
								D	.216	.00300	.020	.71	930		
LOCKHEED ELECTRA	9	17	7450	100	1340	1	.790	M-J	.142	.00489	.042	.80	780	780	
								D	.088	.00291	.035	.90	880		
DOUGLAS XB-7	8.44	20.2	2800	107	1570	1	.921	M-J	.174	.00900	.038	.44	492		TWO-BLADED PROPELLER
								D	.095	.00325	.022	.74	830		
FORD 5AT CENTER ENGINE OFF	10	13.9	9000	85	1340	1	.762	M-J	.154	.00616	.021	.80	598	850	
								D	.090	.00239	.035	.94	700		
FORD 5AT RIGHT ENGINE OFF	9.46	15.8	9375	86	1340	1	.753	M-J	.156	.00350	.029	.90	800	800	
								D	.091	.00300	.031	.83	660		
FORD 5AT LEFT ENGINE OFF	9.46	15.8	5575	94	1340	1	.877	M-J	.291	.00244	.025	.96	842	800	
								D	.085	.00222	.028	.92	800		

M-J ~ METHOD OF THIS THESIS
D ~ " " REFERENCE 3

NOTE: TWO-BLADED PROP. VALUES OBTAINED WITH $\frac{3}{2}Q_n$ FOR T_c FROM FIG. 11 THEN $\frac{2}{3}T_c$ FOR WORKING VALUE

TABLE II.

COMPARISON OF FLIGHT TEST R.P.M. WITH CALCULATED VALUES

LOCKED PROPELLER

The second group of tests was made to find the change in airplane characteristics caused by a propeller locked in various positions. In these tests the propeller hub was rigidly locked to the face plate of the motor stator so the torque developed by the blades could be measured. The two-bladed propeller was locked in three different positions: blades vertical, horizontal, and at 45°. The three-bladed propeller was locked in two positions: one blade vertically down and one blade vertically up. A series of tests were made at the various propeller positions for a given blade angle and the results are shown in Fig. 12 and Fig. 13a,b. The polars in Fig. 12 showed negligible differences for the various positions and for that reason it was thought unnecessary to make tests on all permutations for various blade angles. A closer analysis of the effect of propeller position as presented in Fig. 13a,b. shows that the parasite drag is minimum for the two-bladed propeller locked with the blades horizontal while the three-bladed propeller gives a minimum parasite drag when locked with one blade vertically down.

A complete range of blade angles between 0° and 90° was traversed with the two-bladed propeller locked horizontally and with the three-bladed propeller locked with one blade vertically down. The complete results are plotted in Fig. 14 from which it is apparent that the negative thrust of a locked propeller for both two- and three-blades increases with reduction in blade angle, reaching a maximum at about 10°. The curve for three blades is similar to that for two blades, differing primarily in the higher negative thrusts reached. In Fig. 14a a

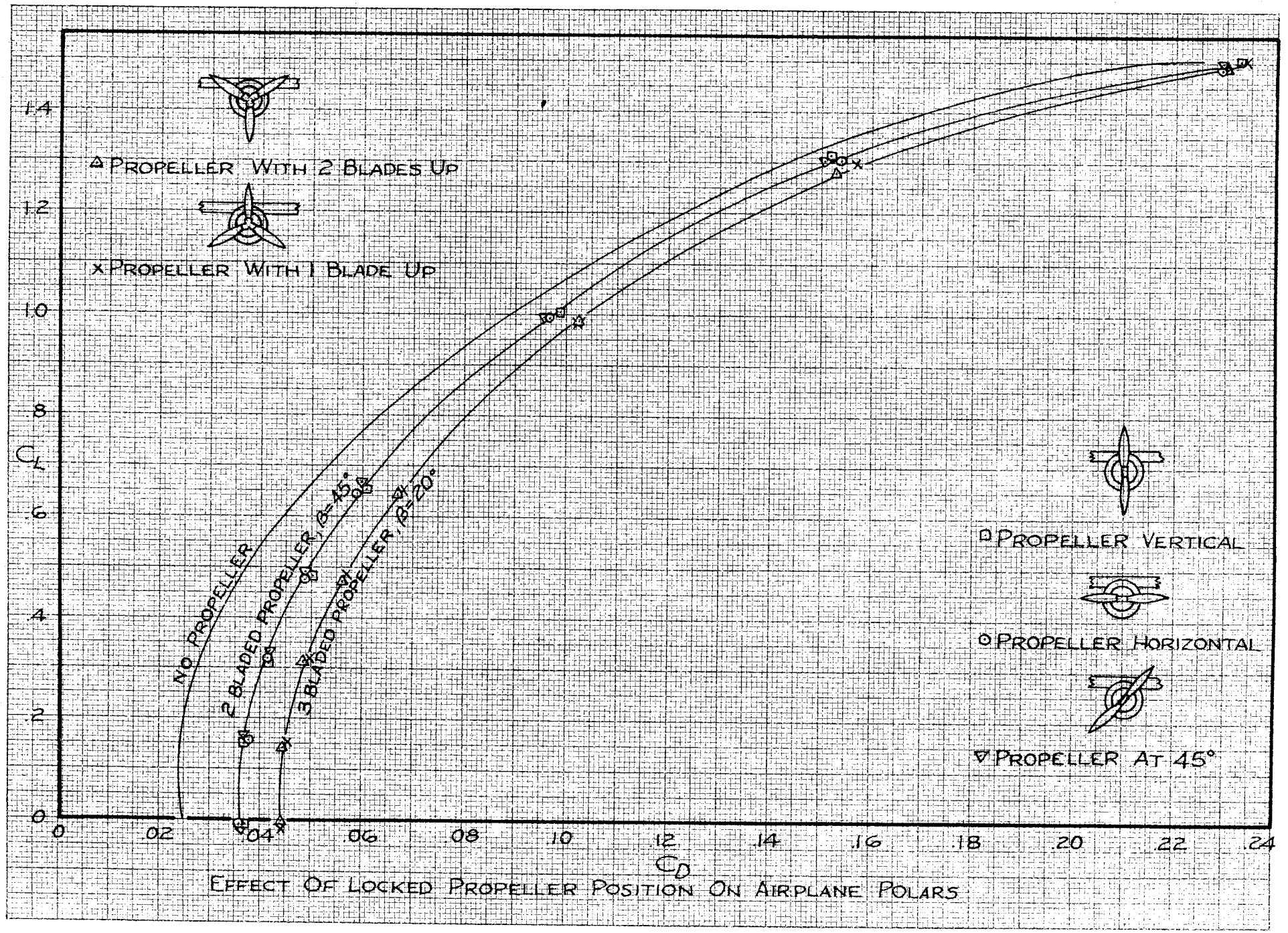

EFFECT OF LOCKED PROPELLER POSITION ON AIRPLANE POLARS

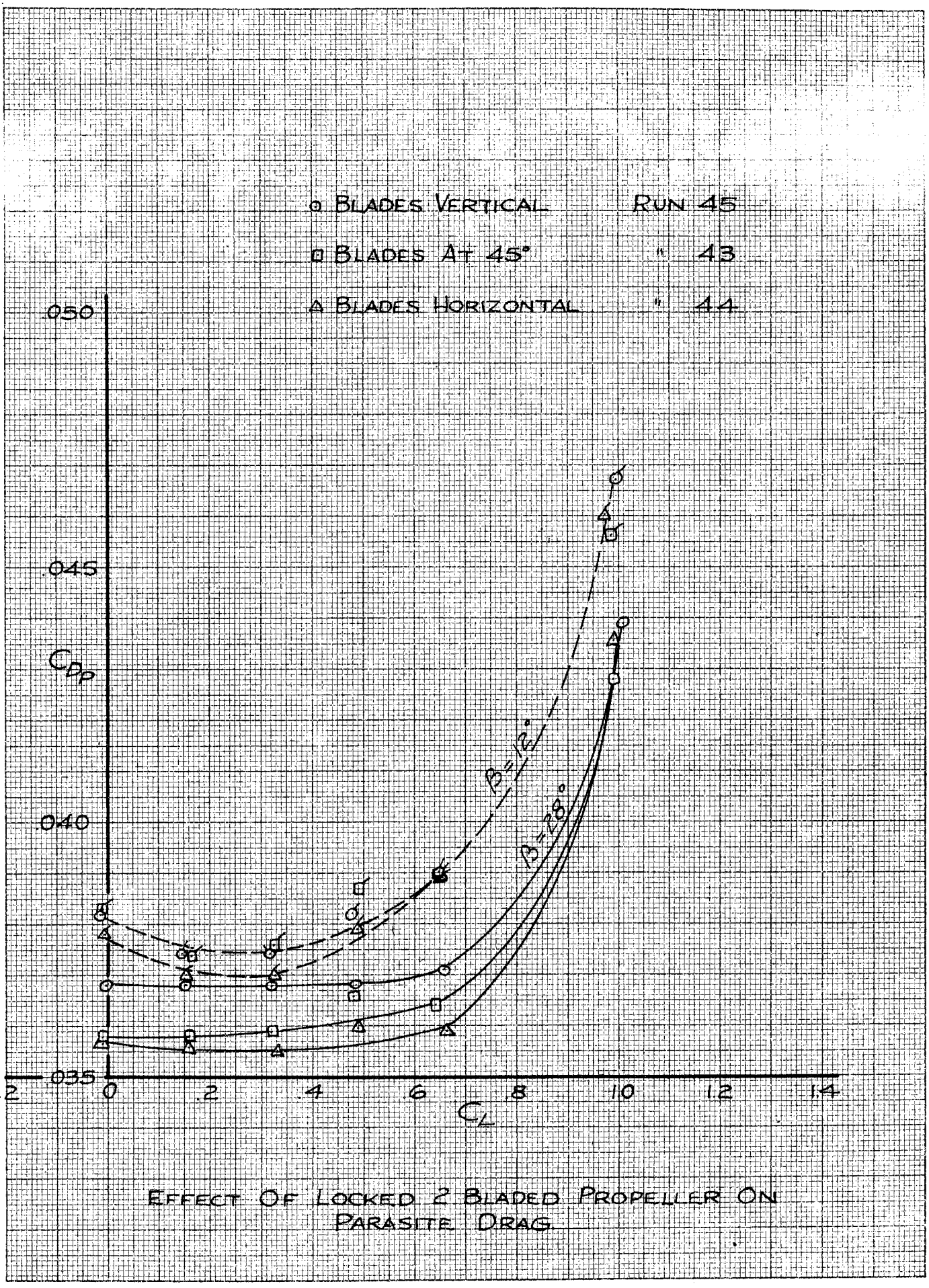

EFFECT OF LOCKED 2 BLADED PROPELLER ON PARASITE DRAG.

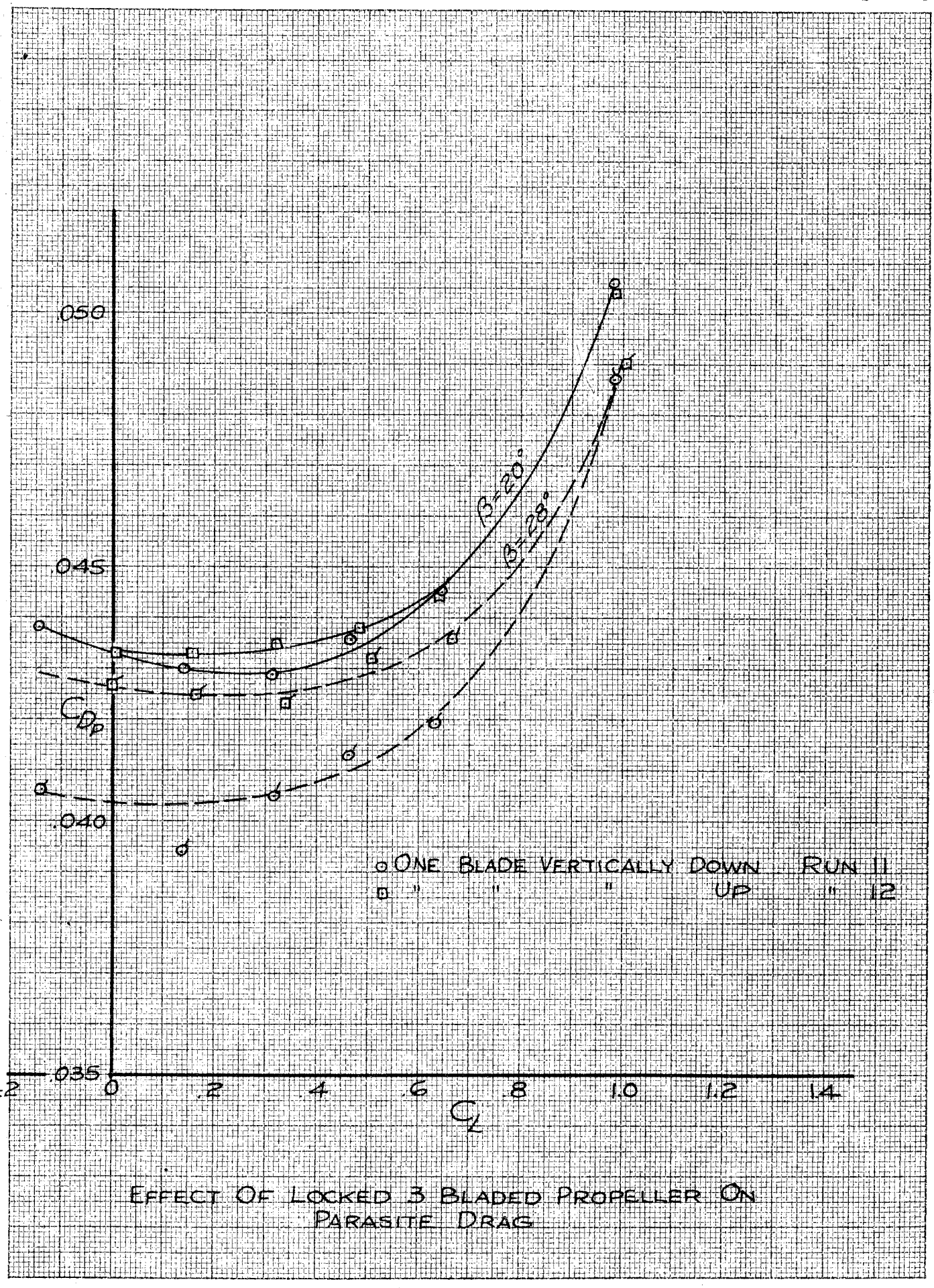

EFFECT OF LOCKED 3 BLADED PROPELLER ON PARASITE DRAG

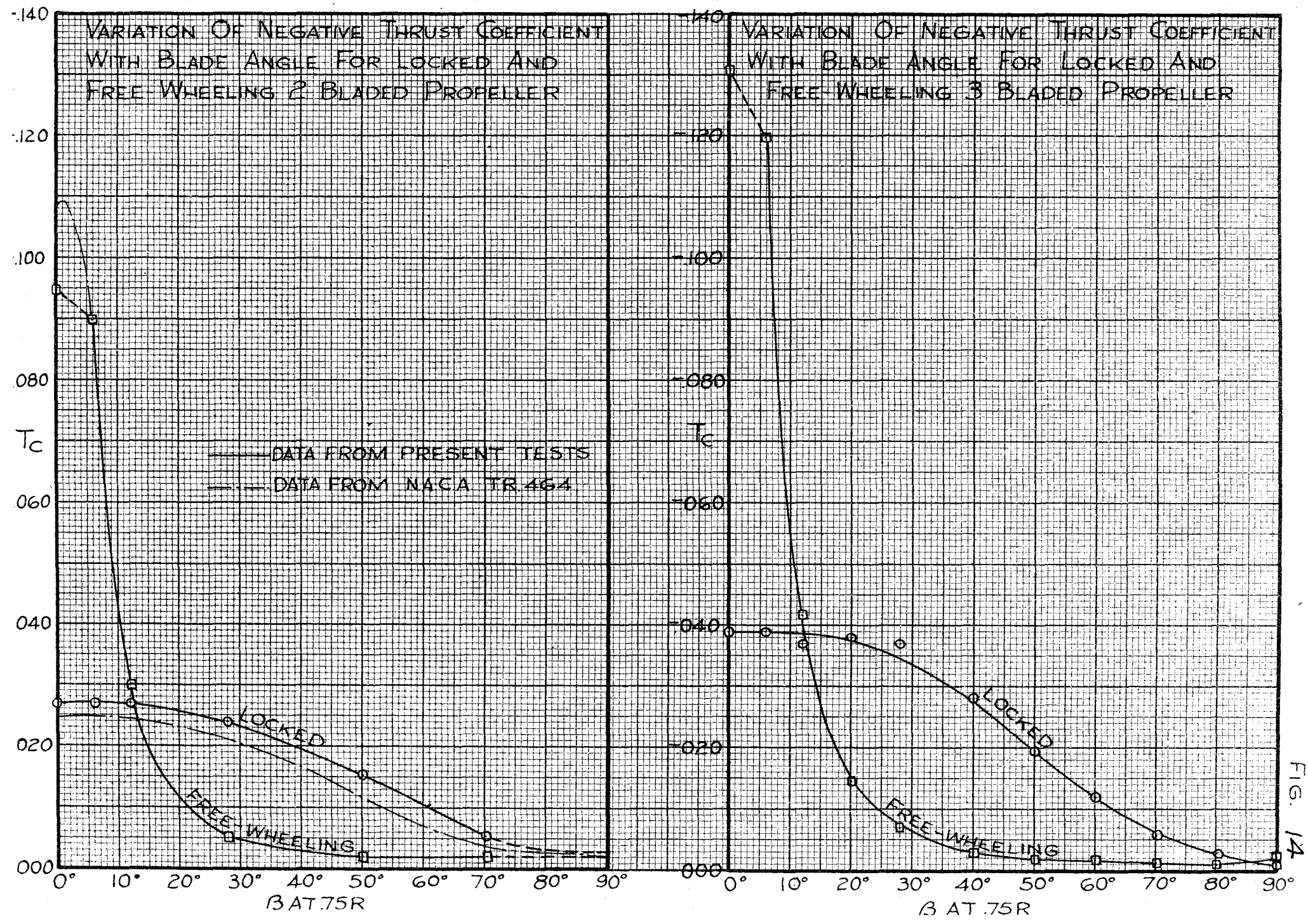

PAGE 25
FIG. 14

comparison is made with data presented in Ref. 1. The lower values of negative thrust given by the latter for the locked propeller can be accounted for by the difference in blade sections and in the solidity ratio of the propeller tested. In Fig. 15 a comparison is made for the three-bladed propeller with data of Ref. 1. The two-bladed propeller data of Ref. 1 was multiplied by 3/2 to obtain the dotted curves shown.

An analytical expression was obtained for the locked two- and three-bladed propellers in terms of the blade angle at .75R and the number of blades of the propeller. This expression consists of a combination of a probability curve and a sine curve the constants of which depend on the propeller design. The expression is of the form:

$$T_c = (.04/e^{.000315\beta^2}) + .002 \sin 3\beta + (B/3 - 1)(90 - \beta).00042$$

where B is the number of blades and β is the blade angle at .75R.

Fig. 16 shows the effect of locked propeller on the airplane three component data. For both two- and three-bladed propeller configurations the drag polar remains the same in shape, moving as a whole in the direction of greater drag as the blade angle decreases. The C_L vs. α curve remains the same in slope, moving slightly to the left with decrease in blade angle. The C_M vs. C_L curves for the two-bladed propeller for blade angles below about 50° show a stabilizing effect due to the propeller. Above 50° a destabilizing effect is apparent. The three-bladed propeller furnishes similar results (Fig. 16b) except that the propeller has a stabilizing effect at all blade angles. The curves of C_L vs. α and C_L vs. C_M plotted show the extreme limits reached by any blade setting.

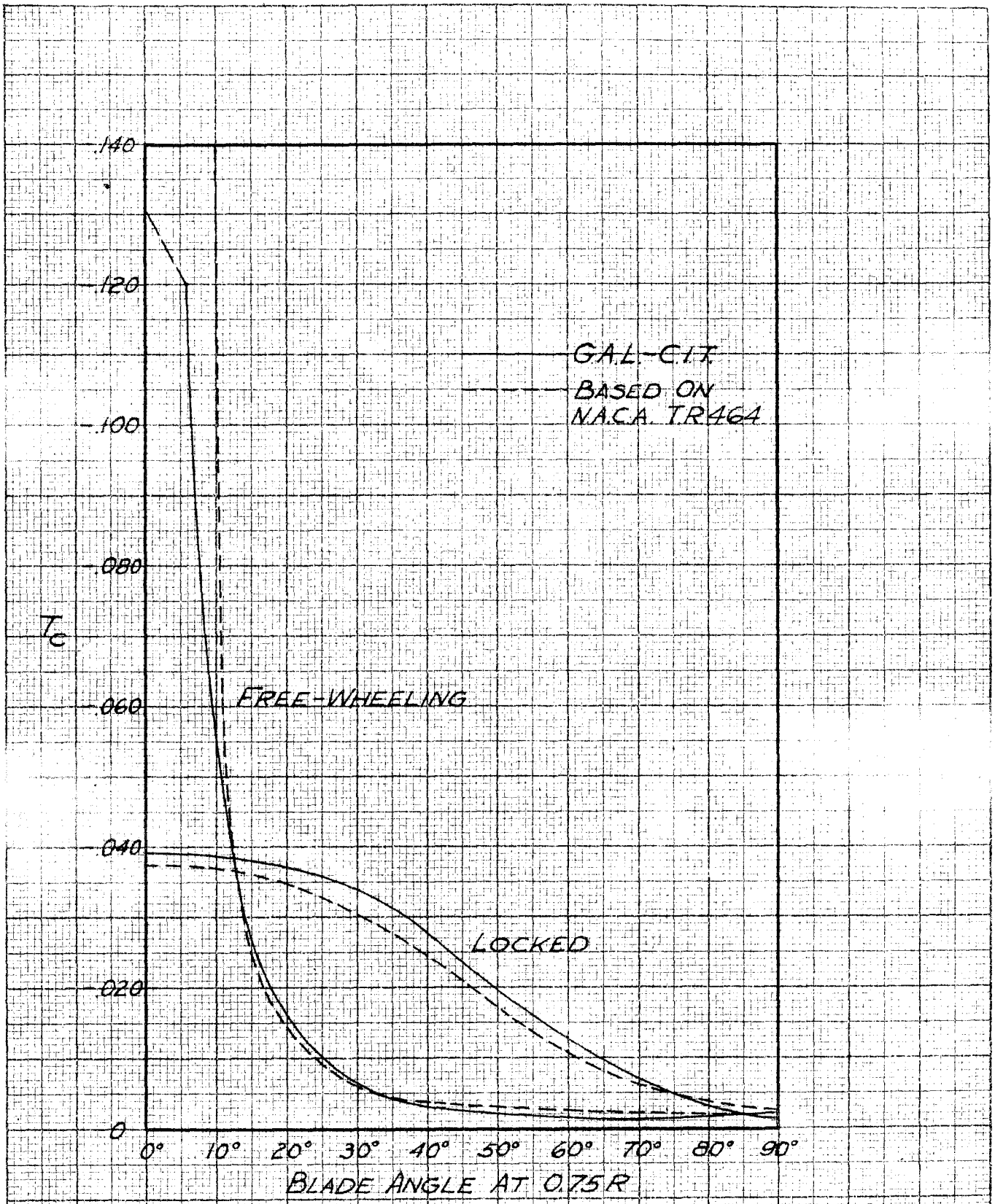

COMPARISON OF G.A.L.-C.I.T. DATA WITH DATA BASED ON N.A.C.A. T.R. 464 FOR LOCKED AND FREE-WHEELING PROPELLER (THREE BLADED PROPELLER)

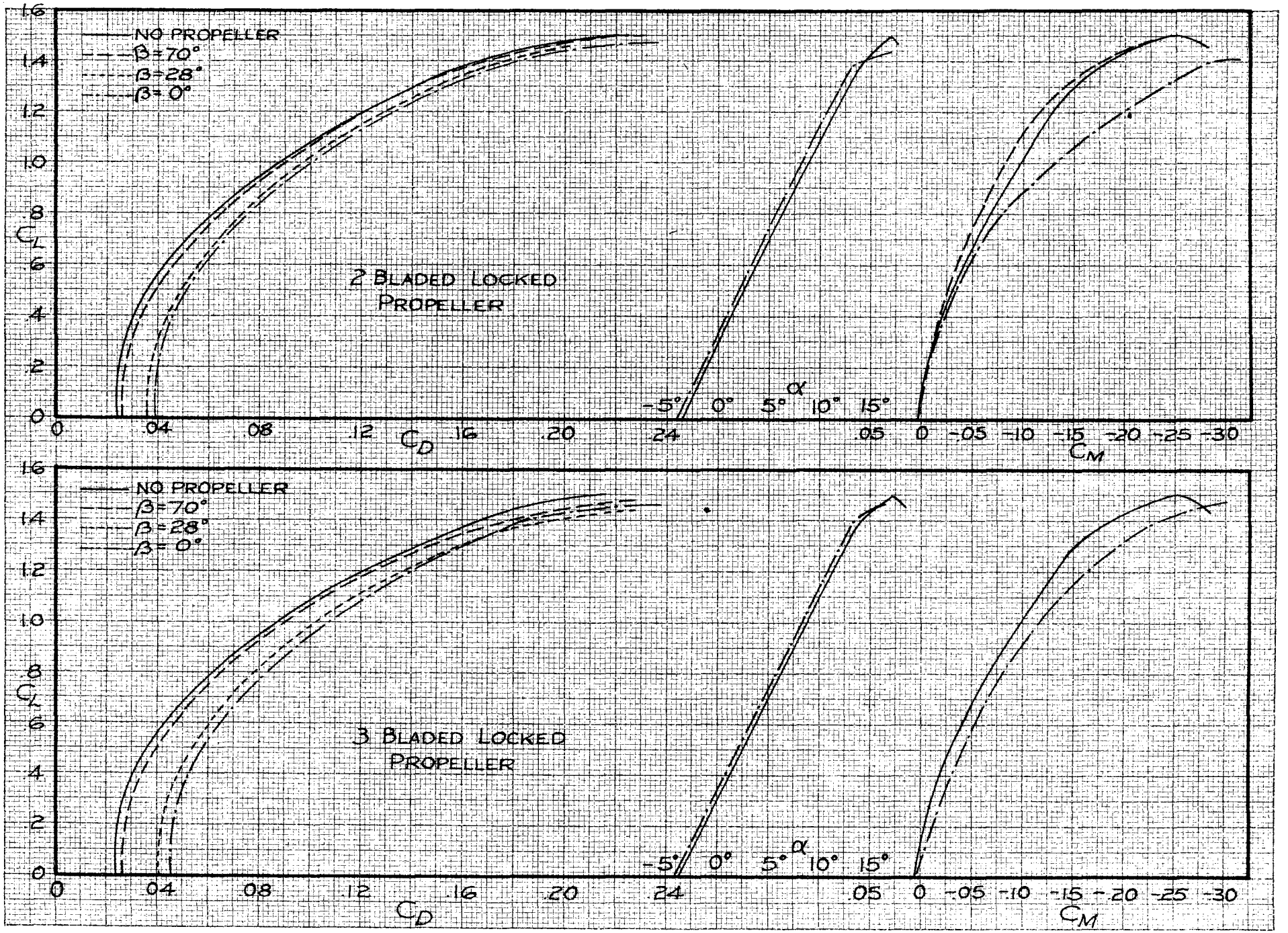

EFFECT OF LOCKED 2 AND 3 BLADED PROPELLERS ON 3 COMPONENT AIRPLANE DATA

FIG. 17

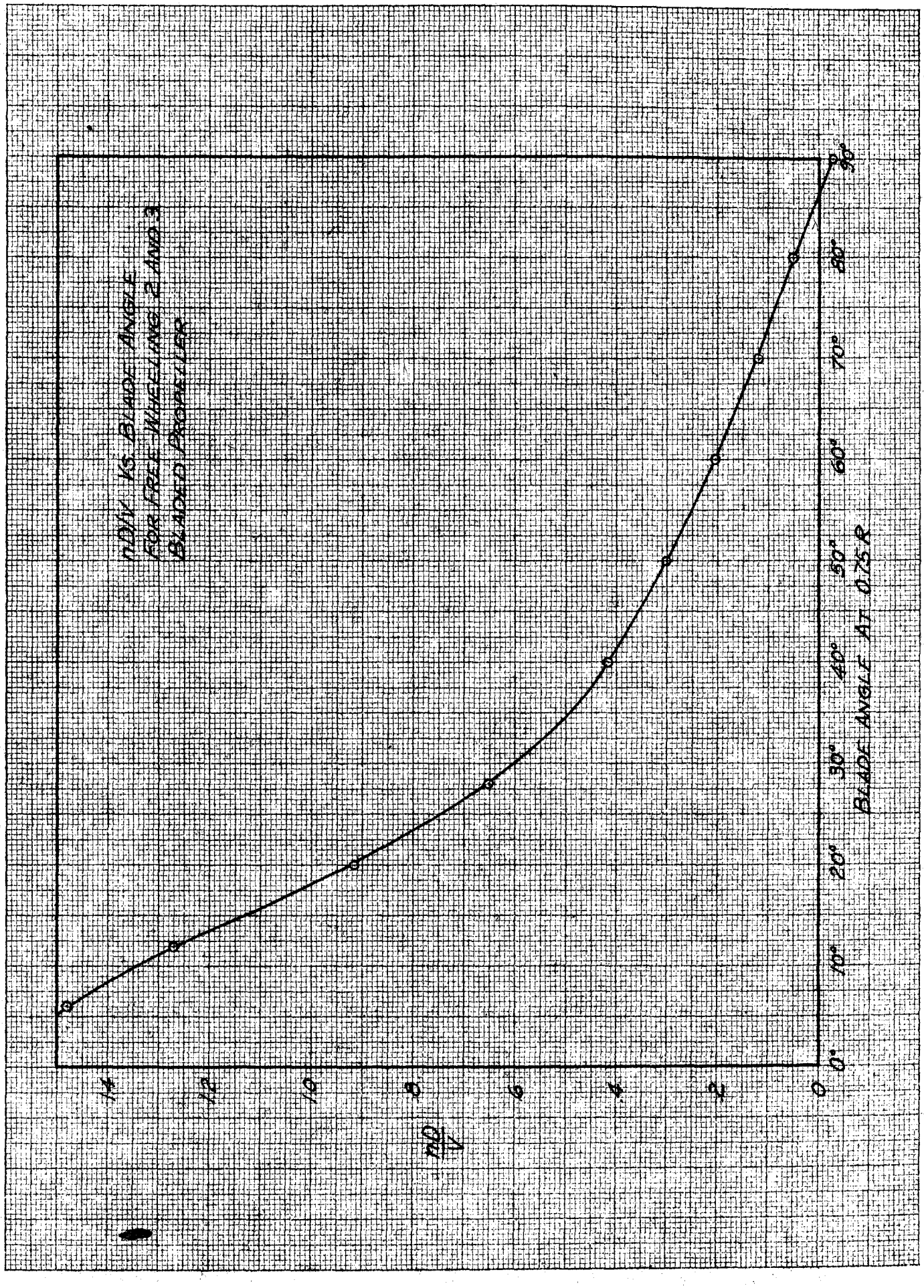
n D/V VS. BLADE-ANGLE
FOR FREE-WHEELING 2 AND 3
BLADED PROPELLER
BLADE ANGLE AT 0.75R
0°
10°
20°
30°
40°
50°
60°
70°
80°
90°
0
2
4
6
8
10
12
14
n D/V

FREE-WHEELING PROPELLER

For the free-wheeling propeller tests, the propeller hub was keyed to the rotor of the motor so that the propeller supplied sufficient torque to overcome the friction of the rotor bearings and counter gears, and the windage loss of the blower. This torque was so small as not to be measurable by the torque meter. Because of the high rotational speeds at low blade angles the wind tunnel velocity was reduced at these angles. The order of magnitude of the rpm. reached by the free-wheeling propeller for any tunnel speed, V, can be calculated from the curve shown (See Fig. 17)

The free-wheeling propeller adds to the drag of the airplane principally by offering additional parasite area and by disturbing the flow over the wing. In the tests the propeller was mounted at a considerable distance from the leading edge of the wing as shown in Fig. 3. For propellers mounted much closer to the wing, as on current multi-engined aircraft, a different effect might be expected.

Fig. 14 shows that for free-wheeling two- and three-bladed propellers, and angle of 30° would be large enough to give practically the minimum deleterious effect on airplane performance. Little advantage would be gained by going to blade angles in excess of 50°. From the three component data plotted in Fig. 18 it is found that the free-wheeling propeller produces similar effects to those mentioned for the locked propeller in Fig. 16 except that unstable tendencies occur at and above about 10° for the two-bladed propeller and about 50° for the three-bladed propeller.

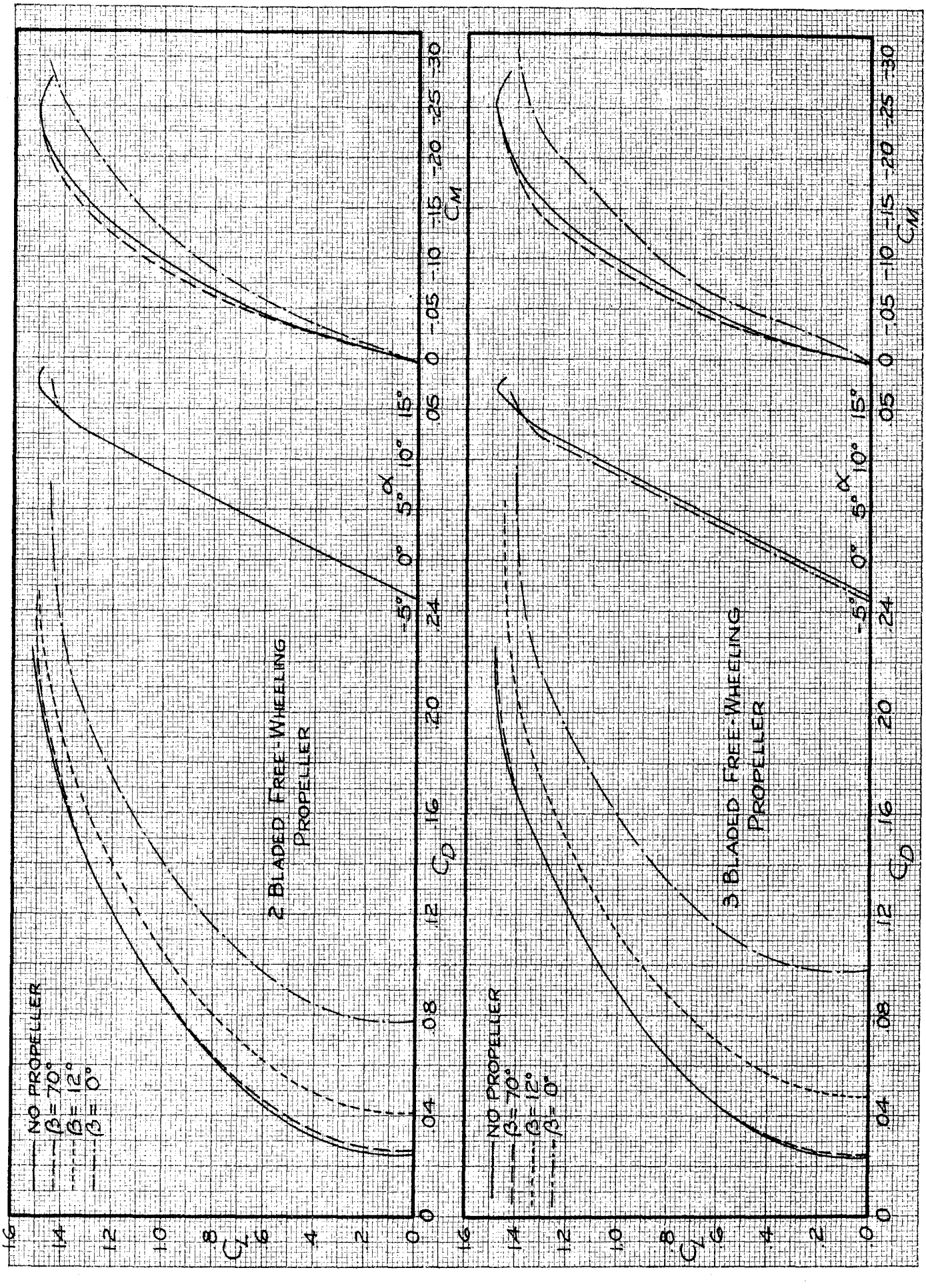

EFFECT OF FREE-WHEELING 2 AND 3 BLADED PROPELLERS ON 3 COMPONENT AIRPLANE DATA

CONCLUSIONS

1. The negative torque and thrust characteristics of a three-bladed propeller are similar to those of a two-bladed propeller, differing in the larger negative maxima reached.

2. The breaking force supplied by a dead-engine can be calculated by the method indicated in this thesis. The formula given should closely approximate actual conditions in view of the considerable amount of friction hp. data upon which it is based.

3. For the high wing monoplane tested an optimum position for the two-bladed propeller is with the blades horizontal, for the three-bladed propeller with one blade vertically down.

4. The negative thrust of a free-wheeling propeller at blade angles above 12^{0} is less than that for a locked propeller.

5. The locked and free-wheeling propeller for high wing monoplanes similar to that tested, produces a shift of the drag polar in the direction of increasing drag, has little effect on the lift and causes a destabilizing effect which is greater with the two-bladed that with the three-bladed propeller.

6. In Table III the negative thrust coefficient, T_c, for different propeller conditions has been tabulated. The values for the angles calculated show that the greatest increase in drag will be obtained from the braked propeller and the minimum increase from the free-wheeling propeller properly set.

The authors wish to thank Dr. Clark B. Millikan for his direction of the research, Dr. A.L. Klein for his supervision of apparatus design, the members of the staff of the Guggenheim Aeronautics Laboratory at the California Institute of Technology for assistance in carrying out this investigation, and the Army, Navy, and various engine manufacturing companied for their generous cooperation in supplying friction horsepower data.

		Two-Bladed Propeller				Three-Bladed Propeller			
Blade Angle		12°	20°	28°	40°	12°	20°	28°	40°
Braked Propeller	$\frac{nD}{V} = .6$	-.045	-.028	-.012	+	-.067	-.044	-.017	+
	$\frac{nD}{V} = .82$	-.050	-.020	+	+	-.074	-.032	+	+
	$\frac{nD}{V} = .95$	-.050	.000	+	+	-.073	-.006	+	+
Locked Propeller		-.027	-.026	-.024	-.019	-.039	-.038	-.035	-.028
F.-W. Propeller		-.032	-.012	-.006	-.003	-.040	-.016	-.008	-.003

NOTE: + INDICATES POSITIVE THRUST COEFFICIENT

TABLE III.

NEGATIVE THRUST COEFFICIENT FOR VARIOUS PROPELER CONDITIONS

REFERENCES

1. Hartman, Edwin P.: "Negative Thrust and Torque Characteristics of an Adjustable-Pitch Metal Propeller". N.A.C.A. Technical Report No. 464, 1932

2. Karman, Th. von and C. B. Millikan: "The Use of the Wind Tunnel in Connection with Aircraft-Design Problems". A.S.M.E. Transactions, March, 1934

3. Douglas, Donald W.: "The Developments and Reliability of the Modern Multi-Engine Air Liner with Special Reference to Multi-Engine Airplanes after Engine Failure." Jour. of the Aero. Sci., July 1935

4. Sparrow, S.W. and Thorne, M.A.: "Friction of Aviation Engines". N.A.C.A. Technical Report No. 262, 1927

5. Russell, J. S. and McCoy, H.M.: "Wind Tunnel Tests on a High Wing Monoplane with Running Propeller". Jour. of the Aero. Sci., Jan., 1936

6. Durand, Wm. F.: "Aerodynamic Theory" Vol. IV, Div. L "Airplane Propellers" by H. Glauert.